Intermetallics 19 (2011) 1479–1488

Contents lists available at ScienceDirect

Intermetallics

journal homepage: www.elsevier.com/locate/intermet

Experimental investigation of the Cu–Si phase diagram at x(Cu)>0.72

Katarzyna Sufryd [a], Norbert Ponweiser [b], Paola Riani [a], Klaus W. Richter [b], Gabriele Cacciamani [a,*]

[a] Dipartimento di Chimica e Chimica Industriale, Università di Genova, via Dodecaneso, 31, I-16146 Genova, Italy
[b] Department of Inorganic Chemistry/Materials Chemistry, University of Vienna, Austria

ARTICLE INFO

Article history:
Received 6 April 2011
Received in revised form
19 May 2011
Accepted 20 May 2011

Keywords:
A. Silicides,various
B. Phase diagrams
F. Diffraction (electron neutron and X-ray)
F. Electron microprobe

ABSTRACT

Cu–Si phase equilibria have been investigated at compositions greater than 72 at.% Cu by X-ray diffraction, optical and electronic microscopy, electron probe microanalysis and differential thermal analysis.

The general aspects of the phase equilibria already reported in literature have been substantially confirmed, but selected composition ranges and the nature of a few invariant equilibria have been modified. In particular stability ranges of the β, δ and η phases have been slightly modified as well as temperature and nature of the invariant equilibria related to the $\gamma \rightleftarrows \delta$ transformation.

Stability of the ε-($Cu_{15}Si_4$) phase has been especially investigated concluding that it is thermodynamically stable but kinetically inhibited by nucleation difficulties which become especially effective when samples are synthesized in very high purity conditions.

Crystal structure and composition ranges of the high temperature β and δ phases, despite difficulties by the non-quenchability of these phases, have been investigated by different methods including high temperature XRD.

1. Introduction

Cu–Si is a key system for several applications: from traditional silicon bronzes to catalysis [1], microelectronics [2] and, more recently, Li-ion batteries [3,4]. On the other hand, Cu–Si phase equilibria, though long investigated, are still known with insufficient detail and affected by some uncertainties, especially about the equilibria involving the β-(Cu,Si), δ-(Cu,Si) and ε-$Cu_{15}Si_4$ phases. For this reason a re-investigation of the Cu-rich part of the phase diagram has been performed.

A comprehensive critical assessment of the Cu–Si literature data up to 1982 was carried out by Olesinski and Abbaschian [5], who presented an assessed version of the phase diagram mainly based on experimental results by Rudolfi [6] and Smith [7–9]. Equilibria among (Cu), κ-(Cu,Si) and γ-(Cu,Si) were especially investigated by Andersen [10], Hibbard et al. [11] and Hopkins [12].

The Cu-Si intermediate phases are located in the Cu-rich part of the diagram, between 5 and 25 at.% Si. The only congruent melting compound, Cu_3Si, is an intermediate solid solution with a small composition range (23–25 at.% Si) and a melting point of 859 °C. For this phase three allotropic modifications denoted as η-Cu_3Si at high temperature, η′-Cu_3Si at intermediate temperature, and η″-Cu_3Si at low temperature have been reported in literature. However, there are uncertainties about the three crystal structures. Solberg [13] investigated the crystal structure of Cu_3Si precipitates on a Si surface by transmission electron microscopy (TEM) and came to the conclusion that these phases are electron compounds based on a trigonally deformed bcc lattice which probably contains a large number of vacancies. The structure was actually first identified as an hexagonal distortion of a bcc lattice [14,15] and Solberg [13] confirmed that this may result when only strongest reflections are considered. Moreover he [13] concluded that η-(Cu,Si) has a disordered structure, while η′-(Cu,Si) and η″-(Cu,Si) are ordered superstructures with η″-(Cu,Si) being a two-dimensional long-period superlattice originating from periodic displacements in η′-(Cu,Si). Additionally, the η″-(Cu,Si) superstructure is expected to vary with composition. More recently Mattern et al. [16] refined the η-(Cu,Si) crystal structure on the basis of high temperature XRD measurements. The same authors observed, in samples annealed at 500 °C, the appearance of superstructure reflections ascribed to the formation of the η″-(Cu,Si) phase, but they were not able to solve the structure.

Three additional high temperature disordered solid solutions have been identified in the Cu–Si system: κ-(Cu,Si), Mg-type, reported at 552–842 °C and 11–14.5 at.% Si; β-(Cu,Si), W-type, reported in a small temperature (785–852 °C) and composition (14–17 at.% Si) range, and δ-(Cu,Si), reported at 710–824 °C and 17.5–19.5 at.% Si, the structure of which was first indexed as tetragonal by Mukherjee et al. [17] and then refined as hexagonal by Mattern [16].

* Corresponding author. Tel.: +39 010 353 6130; fax: +39 010 353 6163.
E-mail address: cacciamani@chimica.unige.it (G. Cacciamani).

0966-9795
doi:10.1016/j.intermet.2011.05.017

Finally, two phases were reported to be stable down to room temperature: γ-(Cu,Si) (also denoted as Cu_5Si), having the *cP*20 β-Mn crystal structure, forming peritectoidally at 729 °C and stable in a narrow composition range (17.2–17.6 at.% Si), and ε-$Cu_{15}Si_4$, (sometimes denoted as Cu_4Si) a line compound at 21.05 at.% Si forming peritectoidally at 800 °C. The ε-$Cu_{15}Si_4$ crystal structure was first identified as cubic with a body centred lattice by Arrhenius et al. [14] and by Morral et al. [18]. Subsequently Mukherjee [17] obtained more X-ray reflections than Morral et al. [18] and concluded that the structure should be cubic but not bcc. Finally, Mattern et al. [16] refined the structure according to a body centred Bravais lattice, claiming, however, to be in agreement with [17].

2. Experimental

Samples have been prepared separately by the groups in Genova and in Vienna, in particular with respect to the investigation of the stability of ε-$Cu_{15}Si_4$ (see below). In Vienna the samples were prepared from copper wire (99.95 and 99.999%, Alfa Aesar) and Silicon lump (99.9999%, Alfa Aesar). The samples, each with a total weight of 1000 mg, were prepared by arc-melting the elements under an argon atmosphere on a water cooled copper plate with a tungsten electrode and a zirconium piece as oxygen getter. In order to obtain proper homogenization, the sample beads were turned over and re-melted at least two times. The weight loss during sample preparation process was smaller than 0.5 mass% and was considered not to affect the sample composition considerably. After preparation the samples were placed in alumina crucibles or wrapped in Mo-foil and sealed in quartz glass tubes under vacuum. Depending on the sample, annealing was carried out at temperatures between 500 and 810 °C for three weeks.

In Genova the samples were prepared from copper sheet (99.999%, Newmet Kock, Waltham Abbey, UK) and silicon granules (99.99, Newmet Kock, Waltham Abbey, UK). The preparation in the arc furnace was the same as in Vienna. The samples were placed in high purity alumina crucibles or wrapped in degassed Mo-foil and sealed in quartz glass tubes under an Argon atmosphere. The annealing took place at temperatures between 500 and 780 °C for time periods ranging from a few days to several weeks.

In both cases the samples were quenched in cold water and prepared for further analysis.

The experimental investigation was carried out using powder X-ray diffraction (XRD) analysis, light optical microscopy (LOM), scanning electron microscopy (SEM) equipped with electron probe microanalysis (EPMA-EDX) and differential thermal analysis (DTA).

For powder X-ray analysis a Bruker D8 ADVANCE system (r = 250.0 mm), equipped with a copper X-ray tube (operated at 40 kV, 40 mA) and a LynxEye position sensitive detector (PSD) was used in Bragg-Brentano reflection setting. The high temperature powder X-ray diffraction was realized with an Anton Paar XRK900 reactor chamber in combination with an automated alignment stage. The samples were smoothly ground in an agate mortar and pressed as approx. 0.5 mm thick layers (15 mm diameter) on the Macor sample holder. The temperature-resolved measurements were performed under evacuated conditions (<5 Pa) from 500(5) to 810(10) °C at different intervals depending on the sample. At each temperature the system was equilibrated for 10 min before a continuous scan over the range 10–100° 2θ with a physical resolution of 0.0103° 2θ. An overall counting time of 2.5 h was performed. The resulting diffractograms for the ambient and the high temperature measurements were evaluated using TOPAS software [19].

Polished sections of the annealed samples were analyzed by LOM using a Leica DM 4000 M and a Zeiss Axiotech 100 microscope. The composition of the coexisting phases and the overall composition of the samples were determined using SEM (Zeiss EVO 40) equipped with an energy dispersive X-ray spectroscopy (EDX, Oxford INCA Energy 300). SEM imaging in backscattered electron (BSE) mode was performed as well. Quantitative EDX analyses were carried out using an acceleration voltage of 20 kV and a counting time of 50 s using a cobalt standard in order to monitor beam current, gain and resolution of the spectrometer. The measured compositions were finally corrected for ZAF (atomic number, absorption and fluorescence) effects using pure elements as standards. The standard deviation for each element was estimated at 0.5 at.% for phase analysis and at 1.0 at.% for global analysis.

DTA measurements were performed on a Setaram Setsys Evolution 2400 (Setaram Instrumentation, Caluire, France) and a Netzsch DTA 404 PC (Netzsch, Selb, Germany) using open alumina crucibles and employing a slow permanent argon flow. A sample mass of approximately 20 mg was used for the experiments. The possible mass loss during the DTA investigations was checked routinely and no relevant mass changes were observed. Using a heating rate of 5 $K \cdot min^{-1}$, two heating and cooling curves were recorded for each sample. The Pt/Pt10%Rh thermocouple (Type S) of the DTA instrument was calibrated at the melting points of pure Sn, Au and Ni.

3. Results and discussion

3.1. Stability of ε-$Cu_{15}Si_4$

The equilibrium Cu–Si phase diagram assessed by Olesinski and Abbaschian [5], based on literature data prior to 1982, includes ε-$Cu_{15}Si_4$ as an equilibrium phase forming peritectoidally at 800 °C from η-Cu_3Si and δ-(Cu,Si). After that, several authors investigated both stability and formation kinetics of this and other Cu–Si intermediate phases, mainly by studying solid state reactions either in diffusion couples or between thin or thick films of the constituent elements.

A number of investigations [20–22] on Cu–Si diffusion couples, reacted at different temperatures between 250 and 550 °C, reported the formation of Cu_3Si but not of γ-(Cu,Si) and ε-$Cu_{15}Si_4$. Similar results were obtained by Levin et al. [23]. They annealed at 470 °C several diffusion couples between Cu and Si, γ-(Cu,Si) and Si, Cu and γ-(Cu,Si), Cu and Cu_3Si, respectively. Analysis revealed the formation of only Cu_3Si in the first two couples, while in the other two couples Cu penetrated along the γ-(Cu,Si) and Cu_3Si grain boundaries caused the fragmentation of the reaction area.

The influence of impurities (especially phosphorous) on the reaction kinetics in Cu–Si diffusion couples was investigated by Van Loo et al. [24,25]. They considered that γ-(Cu,Si) and ε-$Cu_{15}Si_4$ could be absent either for kinetic reasons (which means that the layers are present in principle, but are too small to be observed) or because of impurities (e.g. phosphorous) which change the phase diagram in such a way that γ-(Cu,Si) or ε-$Cu_{15}Si_4$ are not involved any more. Based on their observations they concluded that, being Cu diffusion in γ-(Cu,Si) and ε-$Cu_{15}Si_4$ about 1000 times slower than in Cu_3Si, the virtual absence of γ-(Cu,Si) and ε-$Cu_{15}Si_4$ is mainly due to kinetics and not to impurities.

Solid state reactions between thin or thick films of the constituent elements were also investigated. Stolt et al. [26] prepared Si–Cu bilayers by deposition on thermally oxidized silicon wafers of 100 nm Si layers followed by Cu layers of appropriate thickness in order to obtain the desired composition. After heat treating the bilayers at different temperatures between 200 and 750 °C, they found that in all cases Cu_3Si was the first phase formed, while ε-$Cu_{15}Si_4$ was never formed except in the sample at 20 at.% composition, where it resulted from the reaction between Cu_3Si and γ-(Cu,Si).

Cu–Si bilayers (100 nm Cu layers deposited on thermally oxidized silicon and followed by Si layers of different thickness, between 40 and 120 nm) were prepared by Shpilewsky et al. [27].

Some of them were subjected to implantation of Ar ions. By comparing implanted and non-implanted samples after annealing at different temperatures between 100 and 700 °C they observed that ε-$Cu_{15}Si_4$ is only formed in implanted samples where the maximum density of implanted Ar is close to the Cu/Si interface. They concluded that initiation of ε-$Cu_{15}Si_4$ during irradiation and subsequent annealing may then be attributed to a change in thermodynamic and kinetic parameters of phase formation on ion implantation [27].

Yang et al. [28] deposited Cu layers on a Si(100) substrate in three different ways: by physical vapour deposition (PVD), by ion beam assisted deposition (IBAD) and by a combined method consisting in a thin IBAD film followed by a thicker PVD layer. Samples were investigated before and after annealing at 300 °C. It was found that ε-$Cu_{15}Si_4$ never forms in the PVD samples (which include only γ-(Cu,Si) and Cu_3Si) while it is formed in IBAD samples (even before annealing) and in combined samples, only after annealing at 300 °C. So they concluded that nucleation behaviour of ε-$Cu_{15}Si_4$ is the key factor determining the formation of this phase.

On the other hand, Chromik et al. [29] investigated thermodynamics and kinetics of Cu–Si multi-layers obtained by sputtering alternate Cu and Si thin films on a NaCl substrate. Sputtering rate was controlled in order to form samples with different stoichiometries (those of the Cu–Si intermediate phases) and layer modulation (between 5 and 160 nm). After removing the NaCl substrate samples were subjected to repeated DSC measurements in Al pans by heating them at 10–20 °C/min up to 330–380 °C, annealing 10–20 min at high temperature and cooling. They used high purity elements (99.999 mass%) but unquantified contamination by Ar, H, O, N during sputtering was not excluded [30].

They found that, upon initial heating, Cu_3Si appeared first, while ε-$Cu_{15}Si_4$ and γ-(Cu,Si) were formed at higher temperature (>250 °C). They were not able to obtain ε-$Cu_{15}Si_4$ single phase samples and for this reason they were not able to evaluate its enthalpy of formation.

Moreover, Gillot et al. [31], while studying kinetics of the reactions between CuCl and Si, Si_2Ca, Si_2Fe, Si_2Al_2Ca, $Si_8Al_6Fe_4Ca$ at 200–300 °C, obtained Cu, γ-(Cu,Si) and Cu_3Si phases, but not ε-$Cu_{15}Si_4$.

Table 1
High temperature X-ray powder diffraction of a sample with the nominal composition $Cu_{84.0}Si_{16.0}$, annealed at 500 °C.

Temperature °C	Phase	Amount[a] (%)	Lattice parameters (Å)		Additional reflections	R_{wp}	
			a	*c*	° 2θ		
25	γ	99 (1)	6.2210 (1)			3.64	
	(Cu)	1 (1)	3.622 (1)				
550	γ	85 (1)	6.284 (1)			4.096	
	(Cu)	14 (1)	3.6595 (1)				
	κ	1 (1)	2.5881 (1)	4.2253 (1)			
650	γ	58 (1)	6.296 (1)			4.104	
	(Cu)	3 (1)	3.6674 (1)				
	κ	39 (1)	2.5940 (1)	4.235 (1)			
700	γ	43 (1)	6.3011 (1)			4.221	
	(Cu)	1 (1)	3.6684 (1)				
	κ	56 (1)	2.598 (1)	4.2371 (1)			
750	(Cu)	2 (1)	3.676 (1)			5.17	
	κ	89 (1)	2.604 (1)	4.2401 (1)			
	β	8 (1)	2.894 (1)				
					35.85 (1)		δ[b]
					36.54 (1)		
					43.51 (1)		
					43.90 (1)		
					44.34 (1)		δ[b]
800	(Cu)	3 (1)	3.6815 (1)			3.53	
	κ	62 (1)	2.6064 (1)	4.248 (1)			
	β	35 (1)	2.9234 (1)				
750	(Cu)	3 (1)	3.676 (1)			5.03	
	κ	85 (1)	2.6032 (1)	4.2403 (1)			
	β	12 (1)	2.8932 (1)				
					35.90 (1)		
					36.55 (1)		
					43.51 (1)		
					43.90 (1)		
					44.35 (1)		
550	(Cu)	2 (1)	3.661 (1)			4.707	
	β	12 (1)	2.8741 (1)				
	γ	11 (1)	6.2835 (1)				
	κ	74 (1)	2.591 (1)	4.2245 (1)			
					26.84 (1)		
					36.05 (1)		
					37.20 (1)		
					39.60 (1)		
					51.92 (1)		
25	β	15 (1)	2.5624 (1)	4.184 (1)		5.47	
	γ	9 (1)	6.2223 (1)				
	κ	76 (1)	2.847 (1)				
					27.15 (1)		
					36.50 (1)		
					37.60 (1)		
					39.43 (1)		
					50.31 (1)		

[a] amount calculated on basis if the peak area in the X-Ray powder diffractogram by TOPAS [19].
[b] Peaks are assumed to be related to the formation of the δ-phase.

Finally in a recent work by part of the present authors [32], dedicated to the investigation of the 500 °C Al–Cu–Si phase equilibria, a few Cu–Si binary samples at the ε-$Cu_{15}Si_4$ composition were also investigated. Samples were synthesized by arc melting under Ar atmosphere with zirconium pieces as oxygen getter from silicon granules (99.99 mass%) and copper sheet (99.999 mass%). As cast samples placed inside high purity alumina crucibles or degassed Mo foils were enclosed under vacuum in silica ampoules and annealed for generally one month at 500, 700 and 780 °C. Both as cast and annealed samples did not show ε-$Cu_{15}Si_4$, while it was readily formed in a sample synthesized from lower purity (99.98 mass%) copper.

Experiments independently performed by the group in Vienna provided different results. For this reason the authors decided to merge all the results and start a common investigation of the Cu-rich part of the system, with a special attention to the ε-$Cu_{15}Si_4$ phase and the experimental procedures or conditions which can promote or prevent its formation. Many samples were prepared and exchanged between the two laboratories in order to cross-check results and take advantage from the complementary instrumentation.

As for the formation of ε-$Cu_{15}Si_4$, we observed that it *was not formed*:

a1) In as-cast samples, cooled inside the arc melting furnace,
a2) During cooling in DTA at different cooling rates, generally between 0.5 and 10 °C/min (with one exception discussed later at point b3),
a3) In samples prepared with high purity component elements and annealed for different times (from 4 up to 90 days) in new high purity and smooth containers of alumina or degassed molybdenum,
a4) In selected samples prepared with component elements contaminated by small quantities of other metals (such as Fe and Ca) and annealed for different times in new high purity and smooth alumina containers.

However, we observed that it *was formed*:

b1) In samples prepared with lower purity component elements,
b2) In most samples prepared with high purity component elements and annealed for different times (from 5 h to 20 days) in recycled high purity alumina or non degassed molybdenum containers,
b3) In one sample cooled in DTA at 5 °C/min. The DTA plot was similar to those obtained for similar samples except for a large peak in the cooling curve at about 660 °C, which could be ascribed to the formation of ε-$Cu_{15}Si_4$ in significant under-cooling conditions,
b4) In samples intentionally contaminated with oxygen by sealing them under air (instead of vacuum) prior to annealing.

Selected samples, either with or without ε-$Cu_{15}Si_4$, were analyzed for the presence of light elements such as C, H, N and S using a Perkin Elmer 2400 Series II CHNS/O System Elemental Analyzer. Between 3 and 14 mg of sample material was burned off at a temperature between 970 and 980 °C. The combustion products were analyzed by gas chromatography and quantitatively evaluated. Neither significant quantity of such elements was observed nor significant difference between samples with and without ε-$Cu_{15}Si_4$ appeared.

All our observations suggest that in the prepared samples:

– Contamination by light elements is very low and probably not enough to explain a thermodynamic stabilisation/destabilisation of the phase. However it is not excluded that they can affect the kinetics.
– Contamination by small quantities of other metals (e.g. Ca, Fe) seems not directly related to the formation of ε-$Cu_{15}Si_4$.

Moreover:

– Growth rate seems not the main responsible for ε-$Cu_{15}Si_4$ formation: it was not formed in selected samples after 3 months annealing, but it appeared in other samples after only 5 h annealing at 500 °C.
– The observation that ε-$Cu_{15}Si_4$ was either formed or not formed in samples prepared by the same procedure and in apparently identical conditions suggests that nucleation may be responsible for the phase formation. Actually nucleation

Table 2
High temperature X-ray powder diffraction of a sample with the nominal composition $Cu_{83.6}Si_{16.4}$, annealed at 810 °C. Only the first and the sixth measurements at 810 °C are shown, the other four do not show any significant difference.

Temperature °C	Phase	Amount[a] (%)	Lattice parameters (Å)		R_{wp}
			a	*c*	
25	γ	98 (1)	6.2225 (1)		3.37
	κ	2 (1)	2.5605 (1)	4.1831 (1)	
810	β	91 (1)	2.9215 (1)		4.64
	κ	9 (1)	2.6064 (1)	4.248 (1)	
810	β	90 (1)	2.922 (1)		4.57
	κ	10 (1)	2.6061 (1)	4.2493 (1)	
25	β	4 (1)	2.8455 (1)		
	γ	80 (1)	6.2205 (1)		4.19
	κ	16 (1)	2.5615 (1)	4.1836 (1)	

Table 3
High temperature X-ray powder diffraction of a sample with the nominal composition $Cu_{81.5}Si_{18.5}$ annealed at 780 °C. Only the first and the sixth measurements at 780 °C are shown, the other four do not show any significant difference.

Temperature °C	Phase	Amount[a] (%)	Lattice parameters (Å)		Additional reflections	R_{wp}
			a	*c*	(° 2θ)	
25	γ	99(1)	6.2233(1)			3.56
	ε	1(1)	9.836(1)			
780	δ[a]	100	4.094(1)	5.01(1)		5.46
					36.40(1)	
					38.54(1)	
					43.62(1)	
					43.94(1)	
					48.58(1)	
					49.34(1)	
					51.53(1)	
					75.10(1)	
780	δ[a]	100	4.095(1)	5.01(1)		5.56
					30.81(1)	
					32.38(2)	
					36.42(1)	
					38.55(1)	
					43.50(1)	
					43.90(1)	
					48.56(1)	
					49.32(1)	
					51.41(1)	
					75.05(2)	
25	δ[a]	5(1)	4.0296(1)	4.926(1)		5.19
	γ	93(1)	6.2213(1)			
	κ	2(1)	2.562(1)	4.1824(1)		
					32.63 (1)	
					37.58(1)	
					44.40(1)	
					50.20(1)	

[a] δ according to the structural model of [16].

Table 4
Selection of experimental results used to determine stable phase equilibria.

Sample number	Annealing temperature (°C)	Global composition[a] (at.%Cu)	Phase analysis from EPMA (compositions and amounts) (at.%Cu, volume%)	Phase analysis from XRD (amounts) (volume%)	DTA peaks on heating (on cooling) (°C)	Remarks
1	500	88.0	–	γ (60%) (Cu) (40%)	839 848 945 (943)	$\beta + (Cu) \rightleftarrows \kappa$ $L + (Cu) \rightleftarrows \beta$ $L \rightleftarrows L + (Cu)$
2	500	87.0	–	γ (70%) (Cu) (30%)	822 840 849 923 (921)	$\kappa + \beta \rightleftarrows \kappa$ $\beta + (Cu) \rightleftarrows \kappa$ $L + (Cu) \rightleftarrows \beta$ $L \rightleftarrows L + (Cu)$
3	500	86.5	γ (83.0, 55%) (Cu) (90.0, 45%)	γ (84%) (Cu) (16%)	806 838 844 920	$\kappa + \beta \rightleftarrows \kappa$ $\beta + (Cu) \rightleftarrows \kappa$ $L + (Cu) \rightleftarrows \beta$ $L \rightleftarrows L + (Cu)$
4	500	86.0	–	γ (86%) (Cu) (14%)	734 793 842 849 896 (896)	$\delta \rightleftarrows \kappa + \gamma$ $\kappa + \beta \rightleftarrows \kappa$ $\beta + (Cu) \rightleftarrows \kappa$ $L + (Cu) \rightleftarrows \beta$ $L \rightleftarrows L + (Cu)$
5	650	85.5	κ (86.5, 55%) γ (82.5, 45%)	κ γ		
6	500	85.0	–	γ (89%) (Cu) (11%)	734 782 812 840 852 877 (866)	$\delta \rightleftarrows \kappa + \gamma$ $\beta \rightleftarrows \delta + \kappa$ $\beta \rightleftarrows \beta + \kappa$ $\beta + L \rightleftarrows \beta$ $L + (Cu) \rightleftarrows \beta$ $L \rightleftarrows L + (Cu)$
7	500	84.5	γ (83.0, 90%) (Cu) (90.0, 10%)	–	732 778 805 840 849 884 (883)	$\delta \rightleftarrows \kappa + \gamma$ $\beta \rightleftarrows \delta + \kappa$ $\beta \rightleftarrows \beta + \kappa$ $L + \beta \rightleftarrows \beta$ $L + (Cu) \rightleftarrows \beta$ $L \rightleftarrows L + (Cu)$
8	500	84.0	–	γ (98%) (Cu) (2%)	735 783 830 848 (845)	$\delta \rightleftarrows \kappa + \gamma$ $\beta \rightleftarrows \delta + \kappa$ $L + \beta \rightleftarrows \beta$ $L + (Cu) \rightleftarrows \beta$
9	500	83.5	γ (83.0, 97%) (Cu) (90.0, 3%)	γ (Cu)	733 779 794 820 845 (842)	$\delta \rightleftarrows \kappa + \gamma$ $\beta \rightleftarrows \delta + \kappa$ $\beta \rightleftarrows \beta + \delta$ $L + \beta \rightleftarrows \delta$ $L \rightleftarrows L + \beta$
10	500	83.0	–	γ	733 741 782 821 835 (831)	$\delta \rightleftarrows \kappa + \gamma$ $\delta \rightleftarrows \delta + \gamma$ $\beta \rightleftarrows \delta + \kappa$ $L + \beta \rightleftarrows \delta$ $L \rightleftarrows L + \beta$
11	500	82.0	γ (82.5, 80%) ε (78.0, 20%)	γ ε	735 760 821 826 (815)	$\delta \rightleftarrows \varepsilon + \gamma$ $\delta \rightleftarrows \varepsilon + \delta$ $L + \beta \rightleftarrows \delta$ $L \rightleftarrows L + \beta$
12	500	81.0	γ(82.0, 50%) ε (78.0, 50%)	γ (50%) ε (50%)	736 801 820 827 (815)	$\delta \rightleftarrows \varepsilon + \gamma$ $\eta + \delta \rightleftarrows \varepsilon$ $L \rightleftarrows \delta + \eta$ $L \rightleftarrows L + \delta$
13	760	81.0	γ (δ) (82.0, –) ε (78.5, –)	γ (57%) ε (43%)	–	
14	500	80.0	γ (82.0, –) ε (78.5, –)	ε (78%) γ (22%)	735 800 817 827 (823)	$\delta \rightleftarrows \varepsilon + \gamma$ $\eta + \delta \rightleftarrows \varepsilon$ $L \rightleftarrows \eta + \delta$ $L \rightleftarrows L + \eta$
15	500	79.5	ε (78.0, 80%) γ (82.5, 20%)	ε (78%) γ (22%)	732 799 815 832 (828)	$\delta \rightleftarrows \varepsilon + \gamma$ $\eta + \delta \rightleftarrows \varepsilon$ $L \rightleftarrows \delta + \eta$ $L \rightleftarrows L + \eta$
16	500	79.0	ε (78.0, 98%) η (75.5, 2%)	ε (100%)	801 819 842 (829)	$\eta + \delta \rightleftarrows \varepsilon$ $L \rightleftarrows \eta + \delta$ $L \rightleftarrows L + \eta$
17	500	78.5	ε (78.0, 85%) η (76.0, 15%)	–	618 798 815 845 (837)	$\eta + \varepsilon \rightleftarrows \eta'$ $\eta + \delta \rightleftarrows \varepsilon$ $L \rightleftarrows \delta + \eta$ $L \rightleftarrows L + \eta$
18	500	78	ε (78.5, 75%) η (75.5, 25%)	–	–	

(*continued on next page*)

Table 4 (*continued*)

Sample number	Annealing temperature (°C)	Global composition[a] (at.%Cu)	Phase analysis from EPMA (compositions and amounts) (at.%Cu, volume%)	Phase analysis from XRD (amounts) (volume%)	DTA peaks on heating (on cooling) (°C)	Remarks
19	500	78.0	ε (78.5, 70%) η (75.0, 30%)	ε η	802 821 855 (842)	$\eta + \delta \rightleftarrows \varepsilon$ $L \rightleftarrows \delta + \eta$ $L \rightleftarrows L + \eta$
20	780	77.5	ε (78.5, 70%) η (76.0, 30%)	ε η	–	
21	500	77	–	ε η	670 844 861 (840)	$\eta + \varepsilon \rightleftarrows \eta'$ $L + \eta \rightleftarrows \eta$ $L \rightleftarrows L + \eta$
22	500	72.5	η (76.0, 90%) (Si) (1, 10%)	η Si	554 807 839 (828)	$\eta \rightleftarrows \eta' + \mathrm{Si}$ $L \rightleftarrows \mathrm{Si} + \eta$ $L \rightleftarrows L + \eta$

[a] This is the nominal composition of the prepared samples. For selected samples the global composition measured by EPMA resulted to be equal to the nominal composition, within the EPMA error limits.

rate may be favoured by small, not controllable quantities of compounds formed by light elements (such as oxides, carbides, etc. acting as nucleation seeds) and by large undercooling.

Then, it may be concluded, also in agreement with most of the available literature information, that ε-$Cu_{15}Si_4$ is most probably thermodynamically stable, but kinetically inhibited, mainly due to nucleation difficulties.

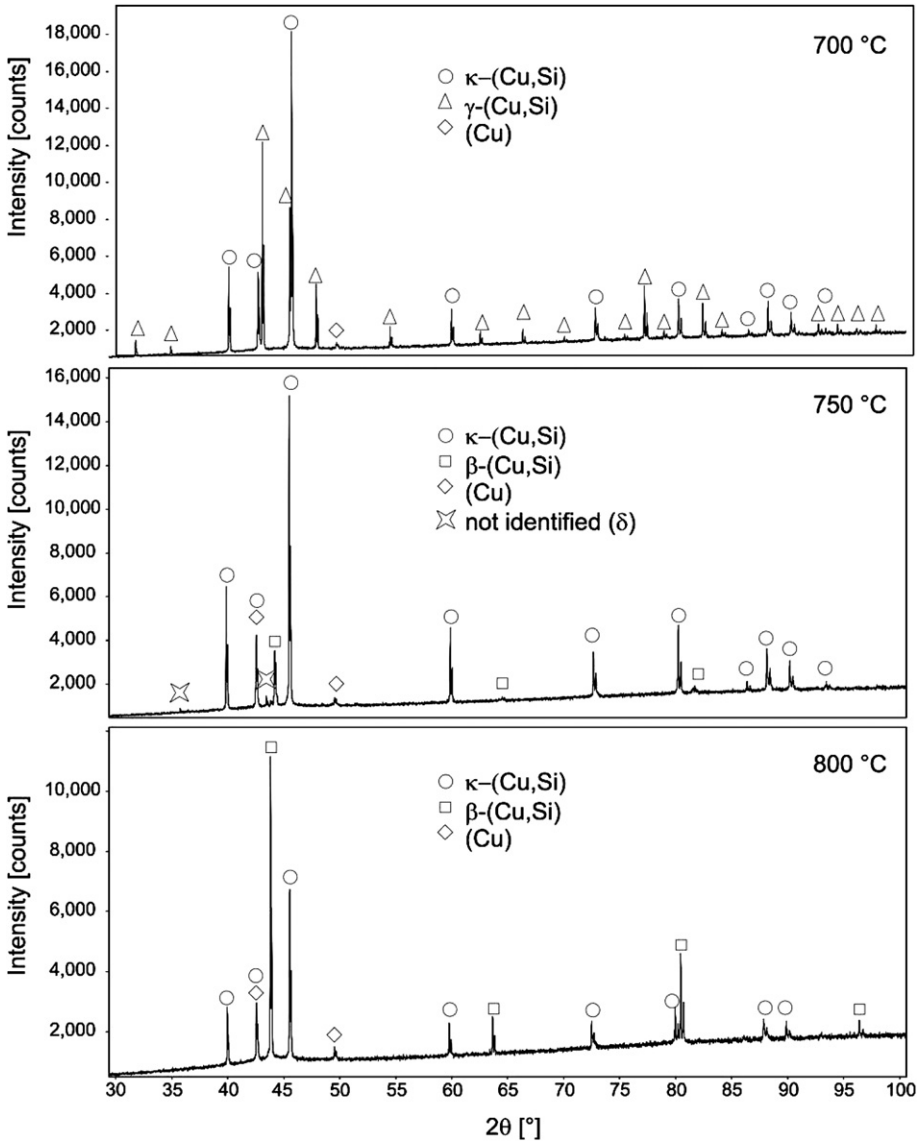

Fig. 1. Comparison of high temperature X-ray diffractograms of a sample with the nominal composition $Cu_{84}Si_{16}$ obtained at different temperatures.

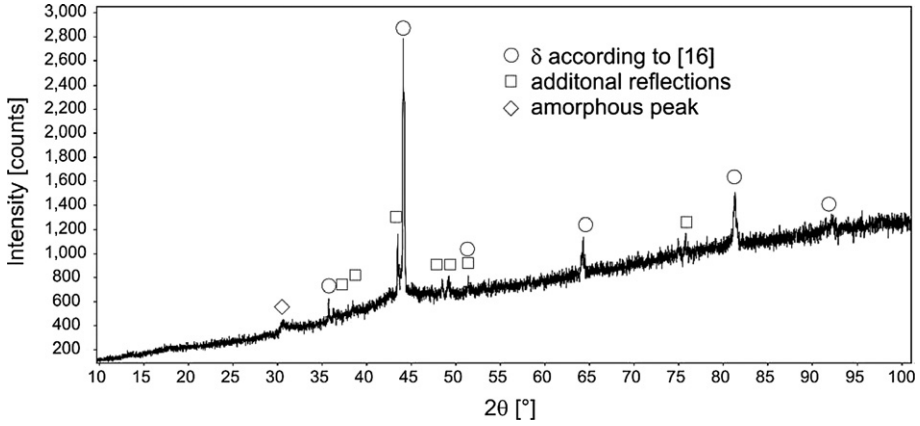

Fig. 2. Powder X-ray diffractogram of a sample with the nominal composition $Cu_{81.5}Si_{18.5}$ at 780 °C.

3.2. High temperature phases β and δ

3.2.1. The β-phase

According to the assessed phase diagram [5] the β-phase (*Im*-3*m*, W-type) with composition between 82.8 and 85.8 at.% Cu is supposed to be stable between 785 and 852 °C. The authors in [5] refer to the work of Isawa [33] (written in Japanese), but do not give any detailed information on the performed experiments.

In the present study, the authors tried to confirm the structure of β-(Cu,Si) from samples with the nominal composition $Cu_{83.7}Si_{16.3}$ and $Cu_{84.1}Si_{15.9}$. These samples were annealed at 810 °C for 21 days and subsequently quenched in water. X-ray powder diffraction analysis showed single phase γ-(Cu,Si) for $Cu_{83.7}Si_{16.3}$ and a mixture of γ-(Cu,Si) and κ-(Cu,Si) for $Cu_{84.1}Si_{15.9}$. Thus it was not possible to preserve the β-phase by quenching.

In order to confirm the structure of β-(Cu,Si), additional samples with the nominal composition $Cu_{83.6}Si_{16.4}$ and $Cu_{84.0}Si_{16.0}$ were annealed at 810 and 500 °C, respectively, then quenched in cold water and finally analyzed by means of high temperature powder X-ray diffraction. Sample $Cu_{84.0}Si_{16.0}$ was analyzed at room temperature and at 550, 650, 700, 750 and 800 °C (Fig. 1); the same temperatures were chosen to analyze the samples while cooling down. The results of the high temperature X-ray powder analysis of this sample are shown in Table 1. At room temperature the sample shows γ-(Cu,Si) as major phase and traces of (Cu). Between 550 and 700 °C the diffractograms show γ-(Cu,Si), traces of (Cu) and an increasing amount of κ-(Cu,Si). This is in good agreement with the proposed stability range of κ in the assessed phase diagram. At 750 °C additional peaks appear which disappear again at 800 °C and are assumed to be related to the δ-phase (see below). These peaks were fitted with a mathematical model so they do not contribute to the calculated error R_{wp}. The measurement at 800 °C shows β-(Cu,Si), (Cu) and κ-(Cu,Si). When cooling down the sample, at 750 °C the same peaks, which are assumed to be related to δ-phase, reappear. At 550 °C a different set of peaks appears which does not match any of the intermetallic compounds in the system and might be due to oxides formed during the long stay in the sample chamber. Contrary to expectations, a small amount of the β-phase was still present at room temperature, although initially it was not possible to quench this phase. Thus, the assessed formation temperature as well as the

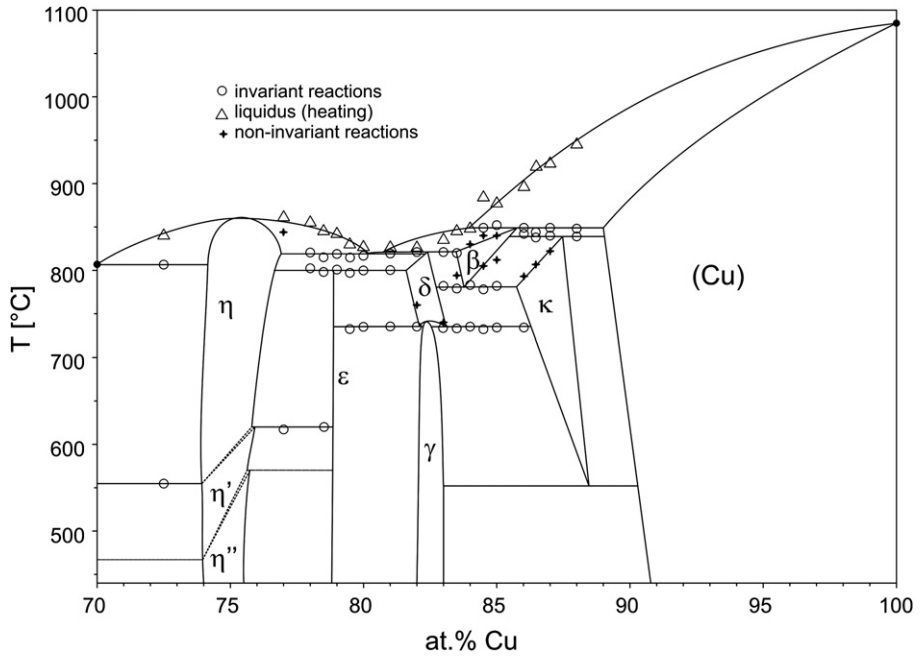

Fig. 3. Equilibrium phase diagram of the Cu–Si system between 70 and 100 at.% Cu with experimental data points from DTA measurements.

crystal structure of the β-phase could be confirmed by the high temperature XRD experiments. The observed inconsistencies are most likely due to surface oxidation of the powder particles during the experiment. The shift in composition (the sample should be single phase β at 800 °C but it was found to contain β and κ) is probably due to the preferred oxidation of Si yielding a shift towards the Cu-rich side. The stabilization of β to room temperature after the experiment may also be related to interaction with oxygen.

In order to improve the results by accelerating the heating process, sample $Cu_{83.6}Si_{16.4}$, annealed at 810 °C, was analyzed at room temperature and then immediately heated up to 810 °C, where every 30 min a total of 6 measurements was performed. Table 2 shows the results of some of the measurements. At room temperature the sample shows γ-(Cu,Si) as major phase and traces of κ-(Cu,Si) are still present. It was again not possible to quench β-(Cu,Si). The measurements at 810 °C show only β-(Cu,Si) in equilibrium with κ-(Cu,Si); no extra phases or peaks occur. Between the first and the 6th measurement no alteration occurs and therefore only these two measurements are shown in Table 2. After cooling down the sample, traces of β-(Cu,Si) still remain present.

Thus, the high temperature XRD experiments confirm the range of existence as well as the crystal structure of the β-phase as given in [5].

3.2.2. The δ-phase

A sample with the nominal composition $Cu_{81.5}Si_{18.5}$ was prepared to study the formation of δ-(Cu,Si) by means of high temperature XRD. The sample was annealed at 780 °C for 21 days and quenched in cold water. Then it was analyzed by XRD at room temperature, subsequently heated to 780 °C where it was analyzed six times by high temperature XRD. Finally it was cooled to room temperature where another diffractogram was taken. The results are shown in Table 3. At room temperature the sample is formed by almost pure γ-phase, ε-(Cu,Si) is found in traces. After heating up to 780 °C, the pattern does show neither γ-(Cu,Si) nor ε-(Cu,Si). We were able to describe major parts of the pattern with the structural model for δ-(Cu,Si) as given by Mattern et al [16]. with the lattice parameters $a = 4.094(1)$ Å and $c = 5.004(1)$ Å, (compared to 4.036 Å and 4.943 Å in [16]). Nevertheless several peaks remain unexplained. The most intense peaks are at 43.62(1) °2θ and 43.94(1) °2θ, the other peaks show very little intensity. It has to be mentioned that the peak at 51.521(1) °2θ matches the position of the (020)-reflex of δ-(Cu,Si) as given by Mattern et al [16], but it was not possible to fit the peak intensity with the Mattern model. Five more measurements were taken at the same temperature, which do not differ from the first except for a broad peak at 30.81(1) °2θ which appears at the second measurement and does not change position or intensity until the last measurement. The results of the sixth measurement are shown in Table 3, too. After cooling down, a final measurement was taken at room temperature. Major phase is again γ-(Cu,Si), κ-(Cu,Si) is present in traces and, against expectations δ-(Cu,Si) is still present, too. Several peaks remain unexplained (see Table 3) which are probably due to oxide formation.

A comparison of the diffractogram of $Cu_{81.5}Si_{18.5}$ at 780 °C and $Cu_{84.0}Si_{16.0}$ at 750 °C (Fig. 2) shows that the observed additional peaks in Table 1 correspond to those observed in $Cu_{81.5}Si_{18.5}$ and can be considered to represent the δ-phase.

The situation can thus be summarized as follows: major parts of the high temperature diffractogram of $Cu_{81.5}Si_{18.5}$ at 780 °C can be explained by the application of the hexagonal structural model given by Mattern [16], but the observation of several additional peaks that appear and disappear at the same temperature suggest that the structural model for δ is not fully correct. However, we were not able to find a unit cell explaining all reflexes observed for δ.

Table 5
Invariant reactions as determined in this work.

Reaction	Temperature (°C)	Phase	Composition (at.% Cu)
$L + (Cu) \rightleftarrows \beta$	849 ± 2	L	84.0 (5)
		(Cu)	89[a]
		β	85.8 (5)
$(Cu) + \beta \rightleftarrows \kappa$	839 ± 2	(Cu)	89[a]
		β	85.5 (5)
		κ	87.5 (5)
$L + \beta \rightleftarrows \delta$	821 ± 2	L	80.8 (5)
		β	83.5 (5)
		δ	82.5 (5)
$L \rightleftarrows \eta + \delta$	818 ± 3	L	80.2 (5)
		η	76.8 (5)
		δ	82.3 (5)
$L \rightleftarrows (Si) + \eta$	807 ± 2	L	70[a]
		(Si)	0[b]
		η	74[a]
$\eta + \delta \rightleftarrows \varepsilon$	800 ± 2	η	76.5 (5)
		δ	81.5 (5)
		ε	78.9 (5)
$\beta \rightleftarrows \delta + \kappa$	781 ± 2	β	83.8 (5)
		δ	83.0 (5)
		κ	85.8 (5)
$\delta \rightleftarrows \varepsilon + \gamma$	735 ± 2	δ	82.1 (5)
		ε	78.9[b]
		γ	82.2 (5)
$\delta \rightleftarrows \gamma + \kappa$	734 ± 2	δ	83.1 (5)
		γ	82.5 (5)
		κ	86.8(5)
$\eta + \varepsilon \rightleftarrows \eta'$	618 ± 3	η	75.8 (5)
		ε	78.9[b]
		η'	75.8(5)
$\eta' + \varepsilon \rightleftarrows \eta''$	570[a]	η'	75.6 (5)
		ε	78.9[b]
		η''	75.6 (5)
$\eta \rightleftarrows (Si) + \eta'$	555 ± 3	(Si)	0[b]
		η	74[a]
		η'	74[a]
$\kappa \rightleftarrows \gamma + (Cu)$	552[a]	κ	89[a]
		γ	83[a]
		(Cu)	90[a]
$\eta' \rightleftarrows \eta'' + (Si)$	467[a]	(Si)	0[b]
		η'	74[a]
		η''	74[a]

[a] Value from literature [5]
[b] Stoichiometric composition

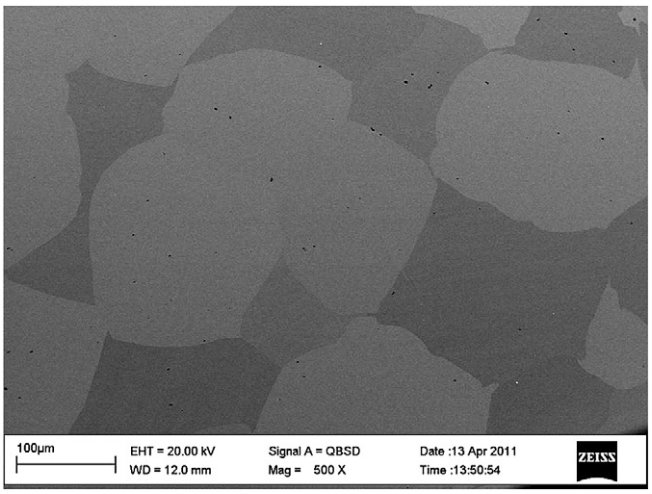

Fig. 4. Microphotograph of sample 20 (78.0 at.% Cu) after 120 h annealing at 780 °C. Dark phase is Cu_3Si and bright phase is ε-$Cu_{15}Si_4$.

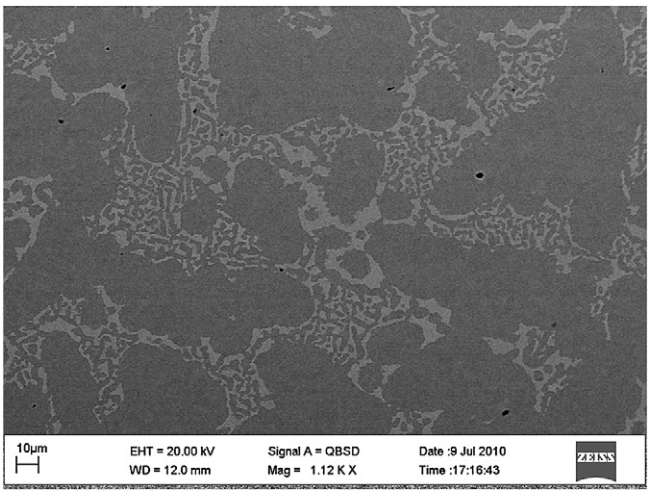

Fig. 5. Microphotograph of sample 15 (79.5 at.% Cu) after 720 h annealing at 500 °C. Dark phase is ε-$Cu_{15}Si_4$ and bright phase is γ-(Cu,Si).

3.3. Phase diagram

More than 50 samples have been prepared and analyzed to investigate Cu–Si phase equilibria in the 72 to 100 at.% Cu composition range. Many of them have been exchanged between the two laboratories in order to cross-check results and to take advantage from the use of the best instrumentation available in both labs. A selection of the most significant and representative results obtained in this work is reported in Table 4. Other results have been obtained which confirm those reported in Table 4 without adding new information: these have been omitted for brevity. Thanks to these results, stable and metastable Cu–Si phase equilibria have been determined. They are presented and commented in the following.

3.3.1. Stable phase equilibria

The equilibrium phase diagram is shown in Fig. 3. Due to the composition of binary compounds in the system the current work is limited to a Cu-content of more than 72 at.%. The phase diagram presented in this work does confirm the general aspects of the phase diagram assessed by Olesinski and Abbaschian [5]. However, several details concerning reaction temperatures, reaction types and homogeneity ranges of selected phases have been modified. An overview of the samples used for determining the phase diagram including a list of the relevant reaction temperatures is shown in Table 4. An overview of the invariant reactions according to this study is given in Table 5.

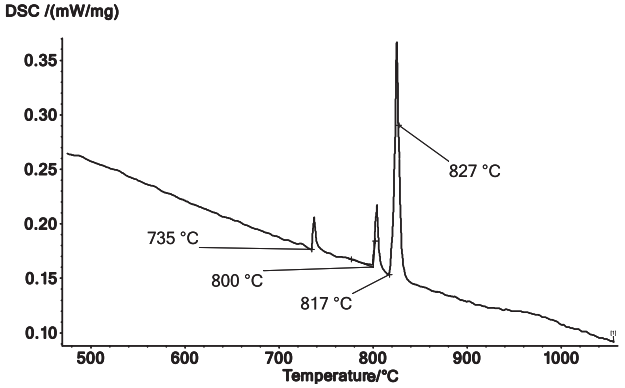

Fig. 6. First cycle of the DTA measurement of sample 14 with the nominal composition $Cu_{80}Si_{20}$.

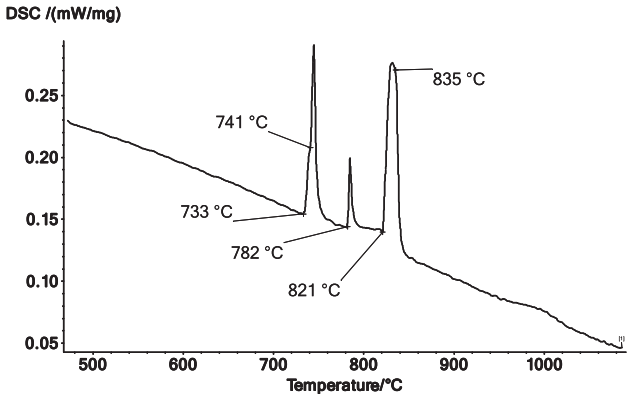

Fig. 7. First cycle of the DTA measurement of the sample 10 with the nominal composition $Cu_{83}Si_{17}$.

Based on EPMA and SEM measurements, the composition of the Cu_3Si phases (η, η' and η'') has been determined ~1 at.% richer in Si compared to the previous phase diagram version. According to DTA measurements the transition from η-Cu_3Si to η′-Cu_3Si occurs at 555 °C in the Si-rich side and at 620 °C in the Cu-rich side of Cu_3Si. It was not investigated if the $\eta \rightleftarrows \eta'$ transition is of first or second order so the transition is drawn as dotted line similar to the phase diagram given by Olesinski and Abbaschian [5]. Two different pieces of sample 22 with the nominal composition $Cu_{72.5}Si_{27.5}$ were annealed at 500 (equilibrium between η' and Si) and 650 °C (equilibrium between η and Si) and then quenched in water. The powder X-ray diffraction of both samples shows exactly the same pattern and the DTA measurements show the same effects at the same temperatures. This indicates that it was not possible to quench the high temperature phase η-Cu_3Si. DTA analysis of the samples show very small thermal effects related to the transition between η' and η. In sample 19 with the nominal composition $Cu_{78}Si_{22}$ the effect was too small to be observed at all.

For the ε-$Cu_{15}Si_4$ phase the stoichiometric composition $Cu_{78.95}Si_{21.05}$ was assumed, instead of the analytical composition $Cu_{78.5}Si_{21.5}$ resulting from the average of the EPMA measurements. The stoichiometric composition is still within the statistical spread of the EPMA measurements and there is no indication of a change in composition in this line compound.

The equilibrium between ε-$Cu_{15}Si_4$ and Cu_3Si is shown in Fig. 4 where a microphotograph of sample 20 (at 78.0 at.% Cu) after 120 h annealing at 780 °C is reported. The large and round ε-$Cu_{15}Si_4$ crystals are due to the high temperature annealing. The peritectoidic formation of ε-$Cu_{15}Si_4$ is confirmed by the

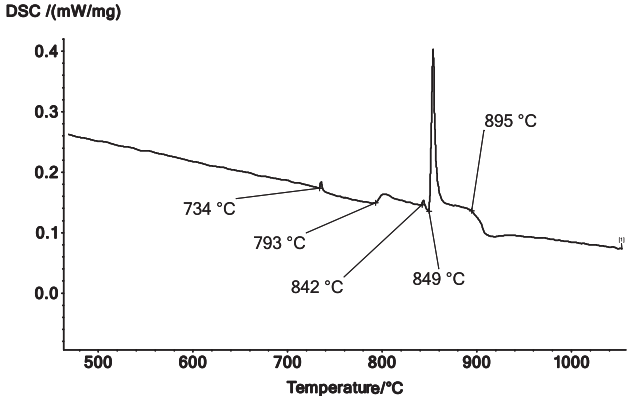

Fig. 8. First cycle of the DTA measurement of the sample 4 with the nominal composition $Cu_{86}Si_{14}$.

microphotograph reported in Fig. 5. It shows sample 15 (79.5 at.% Cu) after 720 h annealing at 500 °C. ε-$Cu_{15}Si_4$, the darker phase, has grown from the δ-(Cu,Si) + η-(Cu,Si) eutectic. Subsequently, during quenching, δ-(Cu,Si) transformed into γ-(Cu,Si) without any appreciable change in composition.

The two invariant reactions $L + \beta \rightleftarrows \delta$ and $L \rightleftarrows \delta + \eta$ are very close concerning their reaction temperature. Nevertheless, the high number of samples showing these reactions allows the determination of the reactions temperatures of 821 and 818 °C, respectively, with reasonable margins of error. The first heating curve in the DTA measurement of sample 14 with the nominal composition $Cu_{80}Si_{20}$ situated in the two-phase field $\varepsilon + \gamma$ is shown in Fig. 6. Three invariant effects including the transition $L \rightleftarrows \delta + \eta$ at 817 °C are labelled. Fig. 7 shows the first heating curve of sample 10 with the nominal composition $Cu_{83}Si_{17}$. The peak with an onset temperature of 821 °C represents the invariant reaction $L + \beta \rightleftarrows \delta$.

Previously, the transition from δ-(Cu,Si) to γ-(Cu,Si) was described to be of peritectoidic type at 729 °C ($\delta + \kappa \rightleftarrows \gamma$) and of eutectoidic type at 710 °C ($\delta \rightleftarrows \gamma + \varepsilon$) [5]. According to the DTA measurements in the present work the transition temperature is essentially the same at both sides of the γ-phase, so the authors assumed a congruent transformation ($\gamma \rightleftarrows \delta$) and two eutectoidic reactions at 735 °C as indicated in Fig. 3. The DTA curve showing the first heating of sample 4 with the nominal composition $Cu_{86}Si_{14}$ is shown in Fig. 8 indicating the reaction $\delta \rightleftarrows \gamma + \kappa$ at 734 °C.

The formation of the β-phase in the reaction $\beta \rightleftarrows \kappa + \delta$ is found in various samples. Furthermore it was possible to determine several non-invariant effects connected with the crossing of phase boundaries involving the β-(Cu,Si) and κ-(Cu,Si) high temperature phases, so the respective phase boundaries could be fixed quite accurately. As an example, the DTA curve of sample 4 with the nominal composition $Cu_{86}Si_{14}$ is shown in Fig. 8. The invariant reactions $L + (Cu) \rightleftarrows \beta$ at 849 °C and $\beta + (Cu) \rightleftarrows \kappa$ at 842 °C show again a very small temperature difference but the two effects are well separated in DTA curves.

Since it was not possible to detect the reaction temperature of the invariant reaction $\kappa \rightleftarrows \gamma + (Cu)$ and the authors of the current work did not find any contradicting results, the temperature (552 °C) and the composition of the reactants are taken from Olesinski and Abbaschian [5]. Similarly, equilibria related to the $\eta'' \rightleftarrows \eta'$ transformation, not detected in this work, were accepted from literature [5].

3.3.2. Metastable phase equilibria

Several samples prepared in the composition range where ε-$Cu_{15}Si_4$ should be stable did not show the phase, but resulted to be constituted by η-(Cu,Si) and γ-(Cu,Si) in various proportions, depending on the global composition. In such samples the composition of γ-(Cu,Si) in metastable equilibrium with η-(Cu,Si) at 500 °C resulted to be about 20 at.% Si, which means about 2 at.% richer in Cu than in the stable phase diagram. On the other hand the composition of η-(Cu,Si) in metastable equilibrium with γ-(Cu,Si) at the same temperature resulted to be about 23.5 at.% Si, only 1 at.% richer in Si than in the stable phase diagram. It was not possible to determine experimentally the metastable equilibria between δ-(Cu,Si) and η-(Cu,Si), due to the non-quenchability of the δ-(Cu,Si) phase. Presumably the composition range of the δ-(Cu,Si) phase is also increased in the Cu-rich side when ε-$Cu_{15}Si_4$ is suppressed.

4. Conclusion

Cu–Si phase equilibria have been investigated at compositions greater than 72 at.% Cu. Stable phases and phase equilibria already reported in literature have been substantially confirmed in their general trends, but selected composition ranges and the nature of a few invariant equilibria have been modified on the basis of our experiments. In particular stability ranges of the β-(Cu,Si), δ-(Cu,Si) and η-(Cu,Si) phases have been slightly modified as well as temperature and nature of the invariant equilibria related to the $\gamma \rightleftarrows \delta$ transformation.

Stability of the ε-($Cu_{15}Si_4$) phase has been especially investigated concluding that it is thermodynamically stable but kinetically inhibited by nucleation difficulties which become especially effective when samples are synthesized from very high purity elements using high purity crucibles.

Investigation of crystal structure and composition ranges of the high temperature β-(Cu,Si) and δ-(Cu,Si) was particularly difficult, due to the non-quenchability of these phases. Stability ranges were determined mainly by DTA, while high temperature XRD was used to investigate crystal structures. The structure of β-(Cu,Si) was confirmed, while for δ-(Cu,Si) some uncertainties still remain.

Acknowledgements

Financial support from the Austrian Science foundation (FWF) under the project number P19305 is gratefully acknowledged. Furthermore, the authors with to thank Christian Lengauer for his support with the high-temperature X-Ray diffraction and Johannes Theiner for the elemental analysis.

References

[1] Parajuli O, Kumar N, Kipp D, Hahm JI. Appl Phys Lett 2007;90:173107.
[2] Liu Y, Song S, Mao D, Ling H, Li M. Microelectronic Eng 2004;75(3):309–15.
[3] Ahn HJ, Kim YS, Kim WB, Sung YE, Seong TY. J Power Sources 2006;163:211–4.
[4] Johnson DC, Mosby JM, Riha SC, Prieto AL. J Mater Chem 2010;20:1993–8.
[5] Olesinski RW, Abbaschian GJ. In: Subramanian PR, Chakrabarti DJ, Laughlin DE, editors. Phase diagrams of binary copper alloys. Materials Park, OH: ASM International; 1994. p. 398–405.
[6] Rudolfi E. Z Anorg Chem 1907;53:216–27 [in German].
[7] Smith CS. J Inst Met 1928;40:359–70.
[8] Smith CS. Trans AIME 1929;83:414–39.
[9] Smith CS. Trans AIME 1940;137:313–29.
[10] Andersen AGH. Trans AIME 1940;137:331–50.
[11] Hibbard Jr WR, Eichelman Jr GH, Saunders WP. Trans AIME 1949;180:92–100.
[12] Hopkins AD. J Inst Met 1953–54;82:163–5.
[13] Solberg BJK. Acta Cryst 1978;A34:684–98.
[14] Arrhenius S, Westgren A. Z Phys Chem B 1931;14:66–79.
[15] Schubert K, Brandauer G. Z. Metallk 1952;43:267.
[16] Mattern N, Seyrich R, Wilde L, Baehtz C, Knapp M, Acker J. J Alloys Compd 2007;429:211–5.
[17] Mukherjee KP, Bandyopadhyaya J, Gupta KP. Trans Metall Soc AIME 1969;245:2335–8.
[18] Morral FR, Westgren A. Ark Kemi Mineral Geol 1934;11:1.
[19] TOPAS, version 3.0. Karlsruhe, Germany: Brucker AXS Inc.; 1999.
[20] Veer FA, Kolster BH, Burgers WG. Trans Metall Soc AIME 1968;242:669.
[21] Onishi M, Muira H. Trans Jpn Inst Met 1977;18:107.
[22] Ward WJ, Carroll KM. J Electrochem Soc 1982;129:227.
[23] Levin L, Atzmon Z, Katsman A, Werber T. Mater Chem Phys 1995;77:4399.
[24] Becht JGM, van Loo FJJ, Metselaar R. In: Barret P, Dufour LC, editors. Reactivity of solids. Amsterdam: Elseviers Publishers B.V; 1985. p. 941.
[25] van Loo FJJ, Vosters PJC, Becht JGM, Metselaar R. Mater Sci Forum 1988;29:261–74.
[26] Stolt L, D'Heurle FM, Harper JME. Thin Solid Films 1991;200:147–56.
[27] Shpilewsky EM, Shpilewsky ME, Andreev MA. Surf Coatings Technol 1995;74-75:937–40.
[28] Yang J, Zhang HB, Tao K, Fan Y. Appl Phys Lett 1994;64:1800–2.
[29] Chromik RR, Neils WK, Cotts EJ. J Appl Phys 1999;86(8):4273–81.
[30] Chromik RR. Personal communication; 2010.
[31] Gillot B, Weber G, Souha H, Zenkouar M. J Alloys Compd 1998;270(1–2):275–80.
[32] Riani P, Sufryd K, Cacciamani G. Intermetallics 2009;17:154–64.
[33] Isawa T. Nippon Kinzoku Gakkaishi 1938;2:400–9.